American Mineralogist, Volume 75, pages 840–846, 1990

Coprecipitation of magnetite and amphibole in black star diopside: A TEM study

N. Doukhan, J. Ingrin, J. C. Doukhan, K. Latrous
Laboratoire de Structure et Propriétés de l'Etat Solide, URA N° 234, Université de Lille-Flandres-Artois, 59655 Villeneuve d'Ascq-Cedex, France

Abstract

A reinvestigation by transmission electron microscopy (TEM) of magnetite and amphibole precipitates occurring in black star diopside from Nammakal (India) underlines the intimate relationships between both types of precipitated phases. A detailed examination shows that the small platelet-shaped crystals of magnetite occur only inside or along the amphibole lamellae. The phases are inferred to have coprecipitated, governed by the diffusion of H into the sample (diopside$_1$ + H_2 → diopside$_2$ + amphibole + magnetite). Such a reaction implies that the amounts of the precipitated phases are completely determined by the initial Al content of the host pyroxene; measurements of these amounts are in quantitative agreement with these predictions.

Furthermore, two families of platelet-shaped precipitates of magnetite are observed; both have epitaxial relations with the diopside matrix such that their larger dimension is approximately parallel to either **c** or **a** of diopside. The angle between the two directions of the magnetite platelets evolves with the size of the precipitates from 103.8° to 105.5°. The phase-boundary thermometer of Fleet et al. (1980) leads to a reaction temperature increasing from 500 to 700 °C. We suggest that the magnetite and amphibole precipitates formed during reheating to this temperature range.

Introduction

Star diopside from Nammakal (province of Tamilnadu, southern India) has previously been described in gemological studies (Marion et al., 1967; Ponahlo, 1968; Schubnel et al., 1968; Woensdregt et al., 1983). The deposit is exploited for the production of cheap gemstones exhibiting asterism somewhat similar to that of star sapphire (Phillips et al., 1981; Samaha, 1982). The asterism is caused by small elongated particles of magnetite in epitaxial relations with the matrix (see Fig. 1; for the theory of optical asterism see Wüthrich and Weibel, 1981). In this study we reinvestigate the dislocations and foreign phases occurring in this material by transmission and analytical electron microscopy (TEM and AEM). Particular attention is devoted to the morphology and to the topology of these foreign phases. Their crystallographic relationships with the matrix strongly suggest that magnetite and amphiboles have precipitated during the metamorphic evolution of the rock. In applying the geothermometer of Robinson et al. (1977) to the orientation relationships between magnetite precipitates and the diopside matrix, one can estimate the precipitation temperature and deduce, at least partially, the path followed by the crystal during its metamorphic history. A reaction is proposed which implies that magnetite and tremolite would have coprecipitated while some H (or water) diffused into the pyroxene matrix.

Optical observations

Thin sections oriented perpendicular to $[010]_{diop}$ and $[\bar{1}01]_{diop}$ of diopside (diop) show two types of lamellae (Fig. 1).

The first consists of platelet-shaped precipitates of magnetite with their larger dimension oriented nearly parallel to either $[001]_{diop}$ or $[100]_{diop}$. Their sizes (measured along the diopside unit cell directions **a**, **b**, and **c** respectively) vary from 8 × 0.5 × 70 to 70 × 5 × 350 μm for the platelets lying approximately along $[001]_{diop}$ and from 50 × 0.5 × 7 to 200 × 5 × 15 μm for the family elongated approximately parallel to $[100]_{diop}$; the proportion of magnetite is estimated to be 0.9 vol%. The coarse magnetite platelets are frequently terminated by thin lamellae parallel to $(010)_{diop}$ (Fig. 1b).

The second type consists of very thin layers of another phase that could not be identified by optical microscopy because of their small size. These layers seem to be parallel to $(010)_{diop}$ and are not observed in the vicinity of the coarse magnetite platelets (Fig. 1b).

AEM observations

An AEM study of this star diopside has been performed from a gemological point of view by Woensdregt et al. (1983). Their observations are confirmed in the present study. However, the present investigation has been carried out with a different point of view: we have tried

0003–004X/90/0708–0840$02.00

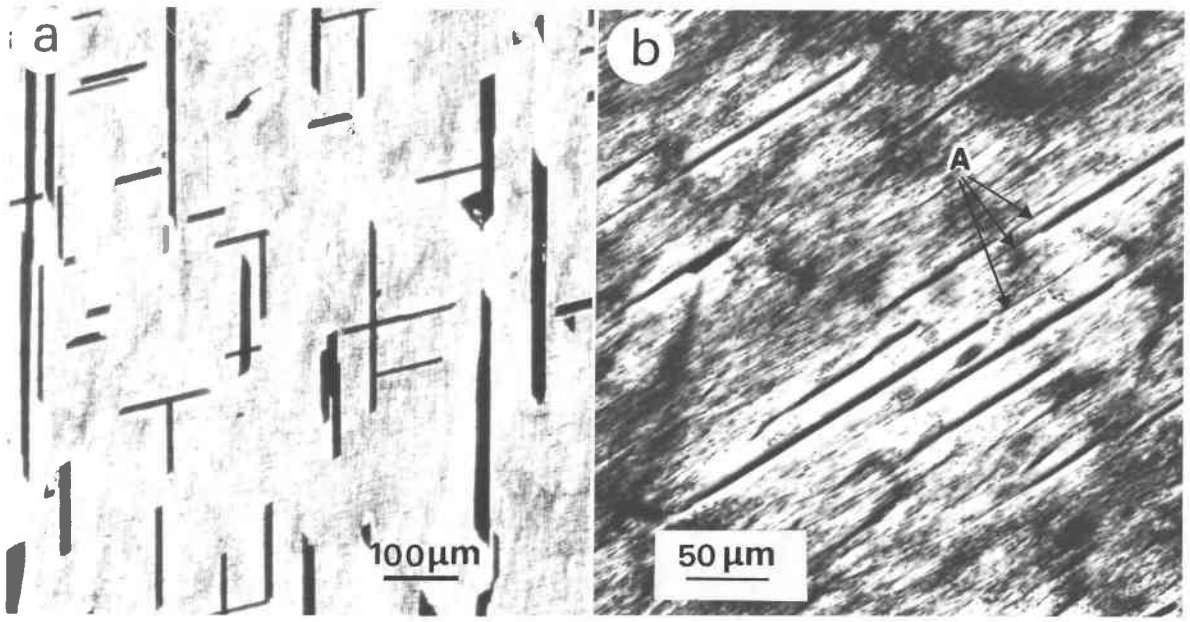

Fig. 1. Thin sections observed by optical microscopy (transmitted light): (**a**) Thin section parallel to $(010)_{diop}$. The dark regions correspond to the large elongated magnetite particles that cause the optical asterism. Their sizes range from approximately 350 μm to a few μm for those visible optically; much smaller ones are detected by TEM. (**b**) Thin section cut perpendicular to the [101] direction; notice the thin lamellae (A) in the plane (010) terminating the magnetite coarse inclusions, and the absence of background contrast close to these magnetite inclusions.

to understand how these foreign phases could have occurred and to decipher at least a part of the thermomechanical history of the rock.

Most of the dislocations detected by TEM are misfit dislocations at the interfaces between matrix and foreign phases; the density of free dislocations is low, and they do not present any specific orientation (see a typical microstructure in Fig. 2). No twins or fractures are observed; if this material was plastically deformed during its metamorphic history, little evidence remains at the microscopic level. The composition of the matrix has been determined by X-ray microanalysis of thin samples rather than by the more precise electron microprobe technique. Indeed, the size of the foreign phases ranges from hundreds of micrometers down to approximately 100 Å (of course these latter small particles are not detected by optical microscopy). The volume analyzed by the electron microprobe technique would therefore probably enclose one or even several particles of foreign phases. The matrix was found to be homogeneous within the uncertainties of this type of analysis; assuming that all the Fe occurs in the form of Fe^{2+}, the composition is $Mg_{0.88}Ca_{0.93}Fe_{0.16}$-$Ti_{0.005}Al_{0.025}[Si_{1.965}Al_{0.035}]O_6$. Except for very slight deviations (slightly lower Ca content, no Na detected) this result is basically similar to the electron microprobe analyses previously reported (Marion et al., 1967; Woensdregt et al., 1983).

The large magnetite precipitates are not easily observed in TEM, probably because the thinning rate of the spinel phase is less than that of diopside, and as a result the magnetite grains remain thick and are not electron transparent. Two types of small precipitates of micrometer size are observed (Fig. 3) and have been characterized by electron diffraction and by microanalysis.

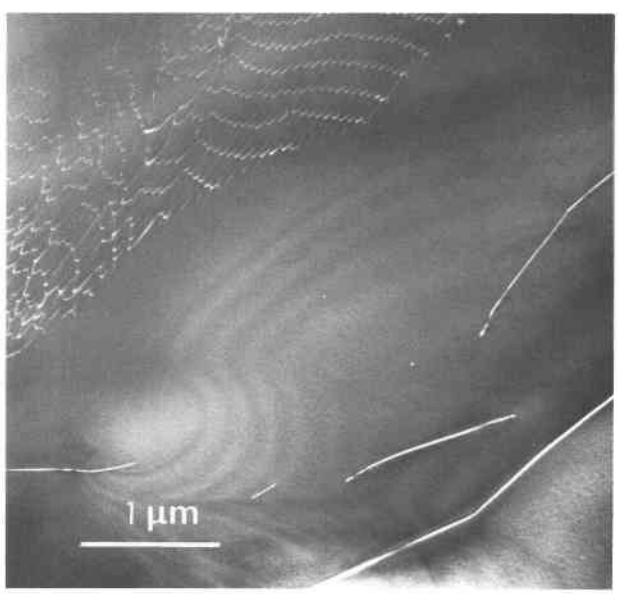

Fig. 2. TEM micrograph of a $(010)_{diop}$ thin foil, weak beam with $\mathbf{g} = 002$; the dislocation network in the upper left region corresponds to the misfit dislocations of a semicoherent amphibole precipitate. In the diopside matrix the dislocation density is much lower, on the order of 10^{10} m^{-2}.

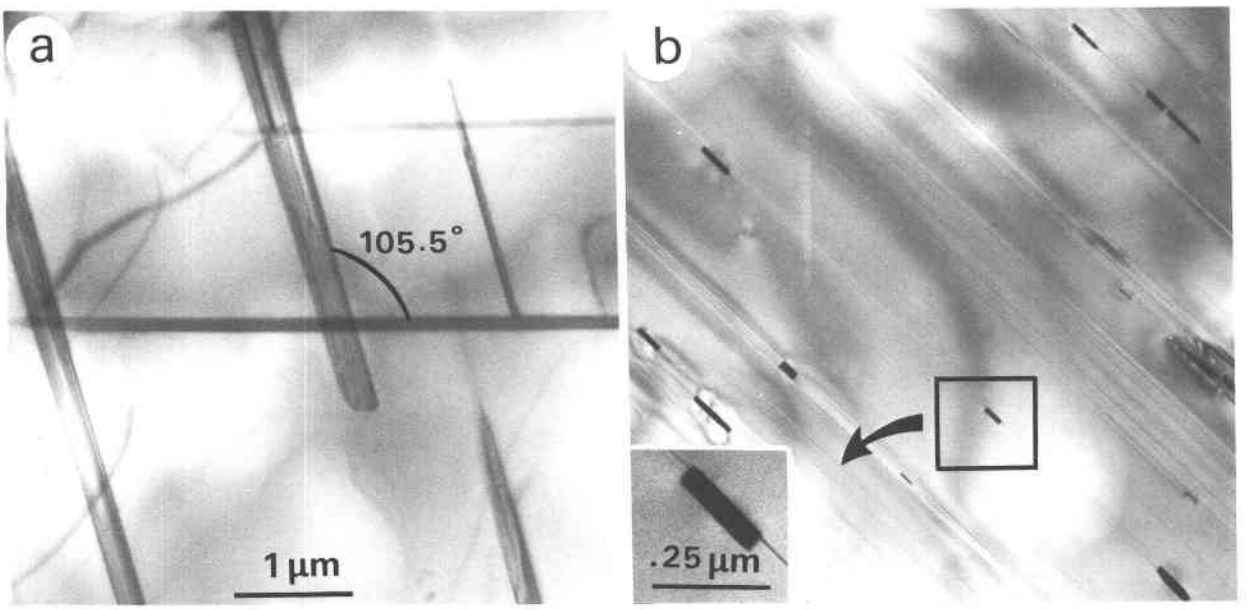

Fig. 3. (**a**) TEM micrograph of a $(010)_{diop}$ thin foil; the two families of platelet-shaped magnetite precipitates lie in this $(010)_{diop}$ plane; they are at ≈8° to the $[001]_{diop}$ and $[100]_{diop}$ directions, and the angle between the long directions of the precipitates is close to 105.5°. (**b**) TEM micrograph of a $(101)_{diop}$ thin foil; the thin amphibole lamellae are seen edge on. The magnetite platelets are inclined to the foil, and they can be put edge on by tilting the specimen. Note that these platelets systematically lie on the amphibole lamellae and are thicker than the associated amphibole lamellae.

The first one is a spinel-family phase with $a \approx 8.4$ Å. Since only Fe is detected by microanalysis, this phase is apparently magnetite, Fe_3O_4 ($a = 8.396$ Å). It occurs as elongated platelets with cross sections varying from 10^{-4} μm^2 to 1 μm^2. These grains clearly present epitaxial relations with the matrix. Their larger dimension is roughly parallel to either $[001]_{diop}$ or $[100]_{diop}$, as for the coarser inclusions observed by optical microscopy. Okamura et al. (1976) have observed similar intergrowths of magnetite lamellae in lunar and terrestrial metamorphic pyroxenes, and they have designated them by Z and X, respectively. We use the same terminology in the following. Diffraction patterns indicate that the lattices of both types are almost perfectly coincident with the diopside lattice along some planes, and the following epitaxial relations hold:

$(010)_{diop} \parallel (011)_{sp}$ for both X and Z types (1)

$(101)_{diop} \parallel (100)_{sp}$ for X type (2a)

$(100)_{diop} \parallel (1\bar{1}\bar{1})_{sp}$ for Z type (2b)

(the subscript sp stands for the spinel-family phase). A detailed examination of the stereographic projections of both structures shows that if $(010)_{diop}$ is exactly superimposed on $(011)_{sp}$ (epitaxial relation 1), only one of the relations (2) can be perfectly fulfilled; a slight rotation of approximately 5° of one of the lattices around their common axis ($[010]_{diop}$ or $[011]_{sp}$) transforms one type of coincidence (for example, relation 2a with a perfect fit for $(101)_{diop}$ with $(100)_{sp}$ but not for $(100)_{diop}$ with $(1\bar{1}\bar{1})_{sp}$) into the other (relation 2b with a perfect fit for $(100)_{diop}$ with $(1\bar{1}\bar{1})_{sp}$). In each case the elastic energy of the misfit boundary is minimum for one interface orientation, and, assuming that these magnetite phases have precipitated in the solid state, the precipitates must have grown in such a way that the direction of their longer dimensions corresponds to this perfect fit. The relative volume of the small magnetite precipitates is easily estimated on TEM micrographs to be slightly less than 0.5% (the thickness of the TEM samples is measured by the contamination technique; see Cordier et al., 1988 for details).

The second kind of small precipitate consists of grains of amphibole that appear as thin, elongated lamellae parallel to $(010)_{diop}$. Their thickness varies from 1 μm to less than approximately 50 Å, the thinnest ones being the most common. They are more or less regularly spaced with a mean spacing of 0.3 μm; the volume of these amphibole crystals, as measured by TEM, represents approximately 3% of the total sample volume. The small magnetite platelets (the ones observed by TEM, which are at most a few micrometers wide) are systematically associated with the amphibole lamellae (Fig. 3). Because of the problem of different thinning rates, it has not been possible to verify whether the large magnetite platelets (the ones observed by optical microscopy) were also systematically associated with amphibole lamellae. However, in a few cases it was possible to observe large amphibole lamellae associated with the larger magnetite platelets (Fig. 4). The chemical composition of the amphibole precipitates is difficult to evaluate because of their thinness. The analyses performed on the larger lamellae

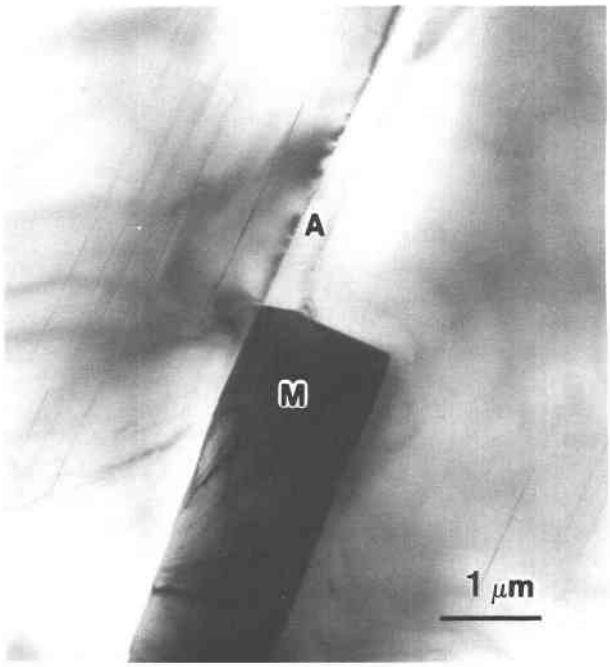

Fig. 4. TEM micrograph showing large amphibole lamellae (A) associated with the larger magnetite platelets (M). Notice the misfit dislocations at the interface between diopside and amphibole; (101) thin foil.

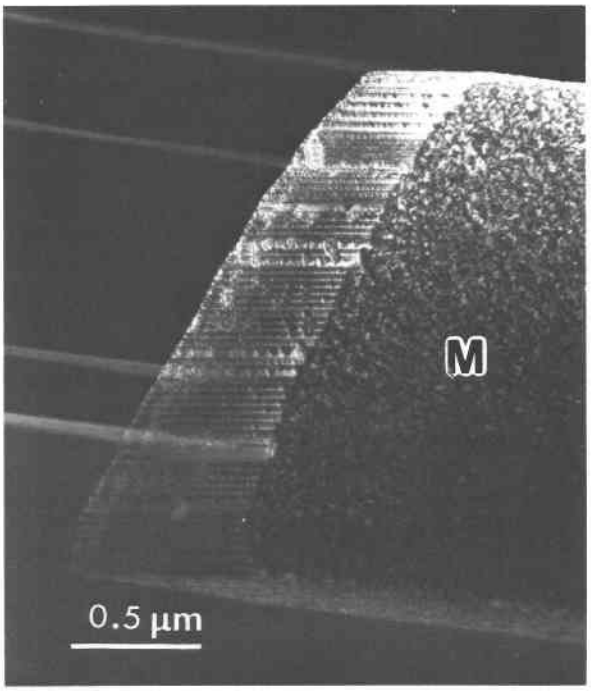

Fig. 5. Misfit dislocations at the interface between diopside and magnetite; (101) thin foil, $\mathbf{g} = 440$.

lead to a composition that can be written, when one takes into account the general rules of site occupancy in the amphibole structures (Hawthorne, 1981), as $Mg_{4.3}Ca_{1.9}Fe_{0.6}Al_{0.2}(Al_{0.2},Si_{7.8})O_{22}(OH)_2$ (no Na^+ detected). The diffraction patterns are consistent with space group $C2/c$, and the corresponding lattice parameters are $a \approx 9.9$ Å, $b \approx 18.1$ Å, and $c \approx 5.3$ Å. All these results are consistent with the amphibole being tremolite. Furthermore, the following epitaxial relations with the diopside matrix were formed:

$$(100)_{diop} \parallel (100)_{trem} \quad (3a)$$

$$(010)_{diop} \parallel (010)_{trem} \quad (3b)$$

The interfaces of the larger lamellae are semicoherent with regular arrays of misfit dislocations in their boundaries (Fig. 4; a similar situation occurs for the larger spinel platelets, see Fig. 5).

Discussion

The epitaxial relations between the precipitates and the diopside matrix strongly suggest an origin of precipitation by homogeneous nucleation for these phases. We thus attempted to determine the temperature range over which the reaction occurred, following the methods of Fleet et al. (1980), and we tried to elucidate the nature of the reaction mechanism as it can be deduced from the TEM observations (chemical compositions, relationships between tremolite and magnetite precipitates, and the volume ratio of tremolite to magnetite, which is equal to 2.0).

Temperature of precipitation

As shown by Fleet et al. (1980), the temperature at which the reaction occurred can be estimated from the orientations of the phase boundaries between magnetite and diopside. The interfacial energy is minimum for certain orientations, and it has been shown in a number of cases that the effect of the stiffness anisotropy can be neglected (Fleet, 1982). The orientations of the minimum-energy interfaces are thus controlled only by minimum-strain considerations. In the case of exsolution of pigeonite or augite in pyroxenes, the lattice parameter b remains unchanged and (010) is rigorously continuous in the monoclinic phases. Fleet et al. (1980) have adapted this model to the case of precipitation of magnetite by using a larger, nonprimitive, monoclinic cell for the spinel-family phase; the corresponding b lattice parameter is very similar (though not identical) to that of the pyroxene matrix. By comparison with the case of exsolution of Ca-poor clinopyroxene in Ca-rich clinopyroxene, they assumed that the orientation leading to a minimum interfacial energy is only a function of the differences between the corresponding pairs of other lattice parameters a, c, and β (Jaffé et al., 1975; Robinson et al., 1971, 1977). The trace Y in $(010)_{diop}$ of the optimal interphase boundary is such that

$$\begin{aligned} Y^2 &= a_1^2x_1^2 + c_1^2z_1^2 + 2a_1c_1x_1z_1\cos\beta_1 \\ &= a_2^2x_2^2 + c_2^2z_2^2 + 2a_2c_2x_2z_2\cos\beta_2 \end{aligned} \quad (4)$$

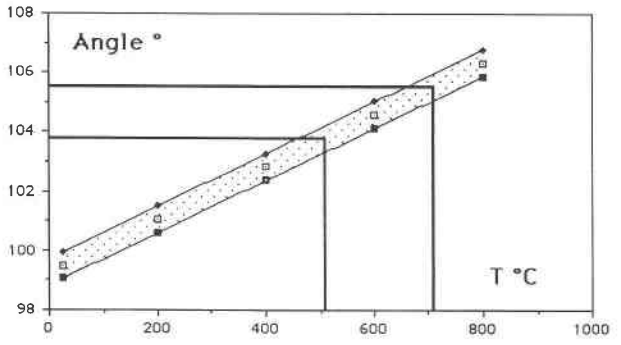

Fig. 6. Variation of the orientation of the precipitates (angle between the Z and X magnetite platelets) with the reaction temperature.

where a_i, c_i, and β_i are the lattice parameters of the matrix and of the precipitate (i = 1 and 2, respectively) and x_i and z_i are the coordinates relative to the corresponding axes ($\mathbf{a}_i$, $\mathbf{c}_i$) of the trace of the interface boundary. At the boundary $x_1 = x_2$ and $z_1 = z_2$. Assuming $z_1 = z_2 = 1$ and $x_1 = x_2 = x$, one obtains

$$(a_1^2 - a_2^2)x^2 + (2a_1c_1\cos\beta_1 - 2a_2c_2\cos\beta_2)x + (c_1^2 - c_2^2) = 0 \quad (5)$$
$$\text{A} \qquad\qquad \text{B} \qquad\qquad \text{C}$$

This second-degree equation has two solutions corresponding to the two types of interface orientation. The smaller $|x|$ leads to an interface near the $(001)_{diop}$ surface; this is the Z-type precipitate; the other solution (a larger $|x|$) corresponds to the X-type precipitate. The angle between the X and Z families of precipitates is given by the formula

$$(Y_1, Y_2) = \text{Arcsin}\left\{\frac{c_1\sin\beta_1}{|Y_1|}\right\} + \text{Arcsin}\left\{\frac{c_1\sin\beta_1}{|Y_2|}\right\} \quad (6)$$

In the present case the magnetite precipitates have the spinel structure (a = 8.396 Å at room temperature) but are described by a larger monoclinic unit cell, with the lattice parameters (labeled mc) at room temperature

$$a_{mc} = 6(d_{sp})_{224} = 10.283 \text{ Å};$$
$$b_{mc} = 3(d_{sp})_{220} = 8.905 \text{ Å}$$
$$c_{mc} = 3(d_{sp})_{224} = 5.142 \text{ Å};$$
$$\beta_{mc} = 180 - [111]_{sp}\Lambda[\bar{1}\bar{1}1]_{sp} = 70.53° \quad (7)$$

The lattice parameters of the diopside matrix that must be compared to the magnetite monoclinic unit cell are defined by **a** = [101], **b** = [010] and **c** = [001]. These parameters can be accurately derived from the trend contours defined by Turnock et al. (1973). Neglecting the effect of minor elements like Ti and Al in the chemical composition of the matrix, one finds at room temperature that a = 9.736 Å, b = 8.936 Å, c = 5.246 Å, and β = 74.63°.

In fact, these values correspond to the observed cpx. The parent cpx had a different composition and therefore different lattice parameters, which can be estimated as follows. The volume proportions of the small precipitates of amphibole (3%) and of magnetite (0.5%) were estimated using TEM micrographs; this allows the composition of the original cpx, before precipitation, to be determined. The general rules for site occupancy in clinopyroxenes lead to the formula $Mg_{0.88}Ca_{0.92}Fe^{2+}_{0.165}Fe^{3+}_{0.015}Al_{0.015}Ti_{0.005}(Al_{0.04}Si_{1.96})O_6$. Considering also the coarser precipitates, the parent pyroxene is predicted to have had the chemical formula $Mg_{0.88}Ca_{0.90}Fe^{2+}_{0.175}Fe^{3+}_{0.035}Al_{0.005}Ti_{0.005}(Al_{0.05}Si_{1.95})O_6$. The difference between the formulas is very small and can be ignored for the determination of the lattice parameters from the trend contours of Turnock et al. (1973).

The thermal-expansion coefficients only of pure diopside have been experimentally determined (Cameron and Papike, 1980). They are used here: $\alpha_{d[100]} = 0.773 \times 10^{-5}$ K^{-1}, $\alpha_{d[001]} = 0.646 \times 10^{-5}$ K^{-1}, $\sin(180° - \beta) = 0.962 \times (1 - 0.145 \times 10^{-5}\,\Delta T)$. For magnetite, the thermal expansion coefficient is $\alpha_{sp} = 1.51 \times 10^{-5}$ K^{-1} (Gray, 1971). The effects of the confining pressure on the lattice parameters are not known precisely, but they are presumably very small and are neglected in the following.

Equations 5 and 6 can be solved numerically. The variation of the angle (Y_1, Y_2) vs. T_{pr}, the precipitation temperature, is shown in Figure 6 for this particular composition with its confidence limits (shaded area), which essentially result from uncertainties in the cell parameters and the expansion coefficients. The angle formed by the X and Z lamellae has been carefully measured on precisely oriented $(010)_{diop}$ thin foils. This angle varies slightly with the size of the lamellae. For the smallest lamellae, it is of the order of 105.5° (with a standard deviation of σ = 1°); this corresponds to a reaction temperature of 720 ± 100 °C (see Fig. 6). For the larger lamellae this angle is 103.8° (σ = 0.5°), and the corresponding temperature is 510 ± 50 °C.

Possible reactions

The problem involves definition of a chemical reaction such that at least one phase nucleating within pyroxene has a non-pyroxene-like composition (e.g., magnetite) with the matrix retaining a normal (i.e., stoichiometric) pyroxene formula. For a pyroxene having the substitution of Al for Si in the tetrahedral sites [compensated by an equivalent amount of trivalent (Fe^{3+}) substitution in octahedral sites], a reaction leading to the precipitation of Fe_2O_3 is found to be

$$(Ca,Mg,Fe^{2+})_{2-2x}Fe^{3+}_{2x}[Al_{2x}Si_{2-2x}]O_6 \rightarrow (Ca,Mg,Fe^{2+})_{2-2x}Al_x[Al_xSi_{2-2x}]O_{3(2-x)} + xFe_2O_3. \quad (8)$$

Fe_2O_3, which occurs only where f_{O_2} is high, would then transform into magnetite Fe_3O_4, whereas the resulting O would be expelled. This is a possible reaction for precipitation of Fe_3O_4. However, such a reaction does not explain the formation of amphibole (often spatially asso-

ciated with magnetite). Furthermore, it requires the diffusion of O over large distances in diopside. The corresponding diffusion coefficient is not very well known (see review in Freer, 1981). Muehlenbachs and Kushiro (1975) report a value of 2.4×10^{-16} m^2 s^{-1} at 1280 °C. If an activation energy on the order of 200 kJmol^{-1} is assumed, a value which is small compared to the activation energy proposed for O diffusion in minerals with comparable crystal structures [like enstatite (389 kJmol^{-1}, Borchardt et al., 1979) or olivine (332 kJmol^{-1}, Jaoul et al., 1980)], the diffusion coefficient of O in diopside would be smaller than 4×10^{-23} m^2 s^{-1} at 500 °C. This is an extremely low value that cannot account for diffusion paths several millimeters long, the size of the crystal. Therefore, reaction 8 cannot describe precipitation of magnetite at moderate temperatures. Furthermore, the TEM observations indicate that the small magnetite precipitates are systematically and epitaxially spatially related to elongated crystals of tremolite. It seems from optical observations that the coarser magnetite platelets are also in contact with coarser (≈ 1 μm wide) and very long amphibole lamellae (such large amphibole lamellae are detected by TEM, but the large magnetite platelets are not; a one-to-one correlation could not therefore be proved). Tremolite nucleation and growth in diopside requires that some H atoms be provided by an external source. A simple reaction for coupled precipitation of magnetite and tremolite would consist of adding water to the system:

$$(Ca,Mg,Fe^{2+})_{2-2x}Fe^{3+}_{2x}[Al_{2x}Si_{2-2x}]O_6 + xH_2O \rightarrow xFe_3O_4 + (1 - 9x/2)\{(Ca,Mg,Fe^{2+})_{2-y}Al_y[Al_ySi_{2-y}]O_6\} + x\{(Ca,Mg,Fe^{2+})_{7-z}Al_z[Al_zSi_{8-z}]O_{22}(OH)_2\} \quad (9)$$

with $y = x(1 - z)/(1 - 9x/2)$. Such a reaction leads to formation of equimolar proportions of magnetite and tremolite. Assuming as an approximation that the O atoms of both phases are closest packed, one expects a volume ratio of tremolite to magnetite close to 6, in disagreement with the measured experimental value, ≈ 2.

Alternatively, H could be provided in the form of H_2, which is known to diffuse rapidly in diopside (see Ingrin et al., 1989; Skogby and Rossman 1989), even at moderate temperature. When one takes into account the coupled reaction $1/2H_2 + Fe^{3+} + O^{--} \rightarrow OH^- + Fe^{2+}$, which allows the incorporation of H into the amphibole phase (Clowe et al., 1988), the resulting reaction would be

$$(Ca,Mg,Fe^{2+})_{2-2x}Fe^{3+}_{2x}[Al_{2x}Si_{2-2x}]O_6 + x/4H_2 \rightarrow 3x/4Fe_3O_4 + (1 - 3x/2) \cdot \{(Ca,Mg,Fe^{2+})_{2-y/4}Al_{y/4}[Al_{y/4}Si_{2-y/4}]O_6\} + x/4\{(Ca,Mg,Fe^{2+})_{7-y}Al_y[Al_ySi_{8-y}]O_{22}(OH)_2\} \quad (10)$$

where $y = 8x/(2 - x)$. In this case the expected volume ratio tremolite/magnetite is approximately 2, in agreement with the experimental data. Furthermore, assuming that all the Fe^{3+} initially contained in the parent diopside has precipitated, the volumes of the precipitated phases are expected to be proportional to twice the initial concentration of Al in the parent diopside. This initial concentration has been estimated to be 0.06 mol per mol of parent diopside; therefore, the expected volume proportion of precipitated magnetite is expected to be 1.5% and that of tremolite 3%. Both values are in good quantitative agreement with observation (1.4 and 3%, respectively).

During this reaction process, H clearly must diffuse over the largest distances. The corresponding diffusion coefficient is not known, but H surely has the greatest rate of diffusion of all species involved in the reaction. The other cations must diffuse over smaller distances on the order of half the mean distance between magnetite precipitates (a few micrometers) for Fe and probably over still smaller distances for Mg, Ca, Al, and Si.

Finally, when one considers the two possible reactions proposed for coupled precipitation of amphibole and magnetite, the reaction involving H diffusion seems to explain much more satisfactorily the relative proportions of the precipitated phases and the low temperature of reaction.

The temperature path as traced by precipitation

The size distribution of the magnetite lamellae into two distinct families (Fig. 1a) suggests that two precipitation events occurred.

The precipitation of coarse magnetite platelets probably occurred at a temperature such that the nucleation rate of the lamellae was low while their growth rate was relatively high. In contrast, the precipitation of many small lamellae (thickness ≤ 1 μm) probably corresponds to a temperature for which the nucleation rate was high, whereas the growth rate was low.

Areas free of small precipitates surrounding the coarser precipitates can be observed systematically. This strongly suggests that these coarse precipitates formed first and that Fe^{3+} was depleted in the surrounding areas over distances of a few micrometers (see Fig. 1b). This process would have prevented subsequent precipitation of small lamellae in those regions. It seems unlikely that the coarse magnetite platelets would have formed by an Oswald ripening mechanism consisting of the coarsening of some lamellae at the expense of the neighboring smaller ones (which would have progressively reverted to pyroxene). The observed size distribution, with two distinct families and numerous very small lamellae, does not correspond to expectations based on this growth mechanism. We believe rather that the event related to the coarse lamellae predated the one associated with the second family of lamellae. In the first section of this discussion, the reaction temperature for the coarse lamellae was estimated to be 500 ± 50 °C, whereas the temperature corresponding to the second event (precipitation of the small lamellae) was estimated to be higher (700 ± 100 °C). Therefore, we suggest that precipitation occurred during a metamorphic reheating event. The reheating event must have occurred rapidly (i.e., the temperature rose quickly from 500 °C to 700 °C) In order to prevent the formation of any platelets of intermediate size. This process may appear to be overly complicated as an explanation for two distinct events; however, we could not find a better explanation. Fleet et al. (1980) have proposed a similar process for formation

of magnetite inclusions in pyroxenes from the Grenville province (Canada).

Conclusions

This AEM-TEM micro-petrographic study clearly shows that the magnetite and amphibole precipitates previously observed in star diopside are coupled. Two distinct generations of precipitates must be considered. The thermometer of Robinson et al. (1977) gives rise to a temperature of precipitation which would increase from 500 °C, for the first family of coarse magnetite lamellae, to 700 °C for the second family of small magnetite precipitates. There are several observations that suggest that the small precipitates postdate the coarser ones, and we suggest that the precipitation occurred during metamorphic reheating.

Finally, it is to be noted that the amphibole lamellae, which can be correctly characterized only by AEM, provide a consistent explanation of the "apparent absence or, at least, the undetected presence of a consistently occurring second inclusion phase" noted by Fleet et al. (1980) in another metamorphic pyroxene rich in magnetite inclusions. The reaction proposed here is fully consistent with all observations, and it implies that the black star diopside was formed in the crust, in contact with a source of gaseous H.

Acknowledgments

We gratefully acknowledge J.C. Van Duysen for his cooperation and for providing access to Edax X-ray microanalysis of the materials department, Centre EDF, 77250 Moret sur Loing. We thank an anonymous referee for his fruitful comments on the lattice misfit theory. This is C.N.R.S.-I.N.S.U.-D.B.T. contribution number 95 (kinetics research program).

References cited

Borchardt, G., Jaoul, O., and Scherrer, S. (1979) Formazione di silicati mediante reazioni allo stato solido ad alta temperatura. La Ceramica, (Nov–Dec), 7–22.

Cameron, M., and Papike, J.J. (1980) Crystal chemistry of silicate pyroxenes. In C.T. Prewitt, Ed., Reviews in mineralogy, vol. 7, Pyroxenes. Mineralogical Society of America, 5–92.

Clowe, C.A., Popp, R.K., and Fritz, S.J. (1988) Experimental investigation of the effect of oxygen fugacity on ferric-ferrous ratios and unit-cell parameters of four natural clinoamphiboles. American Mineralogist, 73, 487–499.

Cordier, P., Boulogne, B., and Doukhan, J. C. (1988) Water precipitation and diffusion in wet quartz and wet berlinite $AlPO_4$. Bulletin de Minéralogie, 111, 113–137.

Fleet, M.E. (1982) Orientation of phase and domain boundaries in crystalline solids. American Mineralogist, 67, 926–936.

Fleet, M.E., Bilcox, G.A., and Barnett, R.L. (1980) Oriented magnetite inclusions in pyroxenes from the Grenville province. Canadian Mineralogist, 18, 89–99.

Freer, R. (1981) Diffusion in silicate minerals and glasses: A data digest and guide to the literature. Contributions to Mineralogy and Petrology, 76, 440–454.

Gray, T.J. (1971) Oxide spinels. In A.M. Alper, Ed., High temperature oxides, vol. 5, North Holland Publishing Co., New York, 219–260.

Hawthorne, F.C. (1981) Crystal chemistry of the amphiboles. In C.T. Prewitt, Ed., Reviews in mineralogy, vol. 9A, Mineralogical Society of America, 1–102.

Ingrin, J., Latrous, K., Doukhan, J.C., and Doukhan, N. (1989) Water in diopside: An electron microscopy and infrared spectroscopy study. European Journal of Mineralogy, 1, 327–341.

Jaffé, H.W., Robinson, P., and Tracy, J.R. (1975) Orientation of pigeonite lamellae in metamorphic augite: Correlation with composition and calculated optimal phase boundaries. American Mineralogist, 60, 9–28.

Jaoul, O., Froidevaux, C., Durham, W.B., and Michaud, M. (1980) Oxygen self-diffusion in forsterite: Implication for the high-temperature creep mechanism. Earth and Planetary Science Letters, 47, 391–397.

Marion, C., Picot, P., and Schubnel, H.J. (1967) Nature des inclusions du diopside noir étoilé de l'Inde. Bulletin de l' Association Française de Gemmologie, 12, 11–12.

Muehlenbachs, K., and Kushiro, I. (1975) Oxygen isotope exchange and equilibrium of silicates with CO_2 or O_2. Carnegie Institution of Washington Year Book, 73, 232–236.

Okamura, F.P., McCallum, I.S., Stroh, J.M., and Ghose, S. (1976) Pyroxene-spinel intergrowths in lunar and terrestrial pyroxenes. Proceedings of the 7th Lunar Scientific Conference, Tempe, Arizona, 1889–1899.

Phillips, D.S., Heuer, A.H., and Mitchell, T.E. (1981) Precipitation in star sapphire I. Philosophical Magazine, A 42, 385–404.

Ponahlo, J.F.R. (1968) Inclusions in black star-pyroxene. Journal of Gemmology, 11, 12–15.

Robinson, P., Jaffe, H.W., Ross, M., and Klein, C.S. (1971) Orientation of exsolution lamellae in clinopyroxenes and clinoamphiboles: Consideration of optimal phase boundaries. American Mineralogist, 56, 909–939.

Robinson, P., Ross, M., Nord, G.L., Smyth, J.R., and Jaffe, H.W. (1977) Exsolution lamellae in augite: Fossil indicators of lattice parameters at high temperature and pressure. American Mineralogist, 62, 857–873.

Samaha, T.G. (1982) Asterism in Sri Lankan corundum. Schweizerische Mineralogische Petrographische Mitteilungen, 62, 15–20.

Schubnel, H.J., Marion, C., and Picot, P. (1968) Die Natur der Einschlüße in schwarzem Stern Diopsid von Indien. Dt Goldschmiede Zeitung, August 1968.

Skogby, H., and Rossman, G.R. (1989) OH^- in pyroxene: An experimental study of incorporation mechanism and stability. American Mineralogist, 74, 1059–1069.

Turnock, A.C., Lindsley, D.H., and Grover, J.E. (1973) Synthesis and unit cell parameters of Ca-Mg-Fe pyroxenes. American Mineralogist, 58, 50–59.

Woensdregt, C.F., Weibel, M., and Wessicken, R. (1983) Electron microscopical investigation of oriented magnetite and amphibole in black star diopside. Schweizerische mineralogische und petrographische Mitteilungen, 63, 167–176.

Wüthrich, A., and Weibel, M. (1981) Optical theory of asterism. Physics and Chemistry of Minerals, 7, 53–54.

Manuscript received June 7, 1989
Manuscript accepted April 17, 1990